IEEE Robotics and Automation Letters (RAL) paper presented at
2024 IEEE/RSJ International Conference on Intelligent Robots and Systems (IROS)
October 14-18, 2024. Abu Dhabi, UAE

A two-chamber soft actuator with an expansion limit line for force enhancement

Jingon Yoon, *Student Member, IEEE*, Junmo Yang, *Student Member, IEEE*, and Dongwon Yun, *Senior Member, IEEE*

***Abstract*— Soft pneumatic actuators (SPAs) that can perform three-dimensional movements are being developed to perform more diverse tasks beyond simple bending. The conventional PneuNet actuators have expansion limit layers, which can obtain more tip force by limiting the expansion of the bottom. However, the presence of the expansion limit layer impedes other motions, such as rotation, when configured with multiple channels. In this study, we propose a two-chamber PneuNet actuator (TPA) to which the expansion limit line (ELLINE) is applied to obtain a force gain without a limitation on rotational motion due to the expansion limit layer. We perform a finite element analysis (FEA) on three designs that can rotate and bend using two-chamber to find the optimal design. The effects on twisting, bending, and tip force according to the width of the ELLINE on the selected design were then verified through an FEA. After measuring rotation and bending for the fabricated actuator with and without the ELLINE. In the case of the fabricated TPA with the ELLINE, the bending decreased by 19.8%. However, rotation increased by 22.8 %, tip force increased by 1.53 times (with the ELLINE the force is 2.77 N in 70 kPa; without the ELLINE it is 1.8 N in 70 kPa), and grasping force increased by 5 times (with the ELLINE the force is 500 gf in 70 kPa, without the ELLINE it is 100 gf in 70 kPa). Furthermore, we fabricated a gripper using three actuators, capable of holding a weight of 505 g and objects of various shapes.**

***Index Terms*— Soft pneumatic actuator, soft robot applications, grippers and other end-effectors.**

I. INTRODUCTION

Unlike rigid robots, which pose safety issues due to collisions with surrounding objects or people [1], soft robots can interact with the environment and operate safely in unexpected contact situations or when handling delicate objects [2]. The actuators used in soft robotics are composed of materials with the following characteristics. First, silicone, which is capable of large strain (>100%), possesses low toxicity and high durability and has a low mechanical damping coefficient [3],[4]. Second, the stiffness and strain rate of shape memory polymers and alloys can be adjusted according to temperature [5],[6]. Third, electroactive polymers, such as dielectric elastomer actuators (DEA) [7], polypyrrole (PPy)-based polymer actuator [8],[9], induce bending when subjected to voltages. Fourth, electrorheological fluids are capable of modulating rheological properties upon the application of an electric field [10]. Fifth and finally, fiber and textile offer a wide range of stretch properties that can produce complex motion in soft actuators [11],[12]. Actuators composed of these operate by pressurization, heating, voltage, electric and magnetic field. Among them, the soft pneumatic actuators (SPAs) are used in various fields, [13],[14] such as underwater robots, [15] hand assistance and rehabilitation, [16],[17] and walking robots [18] because of its simple input, high compliance, and stability through flexibility.

The existing SPAs are used in various fields because automation to provide a notable range of movements and high-power densities. SPAs that can perform three-dimensional movements (bending, twisting, and spiral trajectory) are being developed to perform more diverse tasks beyond simple bending. A fiber-reinforced actuator uses one chamber to control the bending direction by limiting expansion depending on the winding direction of the wire [19],[20]. And PneuNet actuators can be bent in a spiral trajectory by giving an angle to the bellow-shaped channel [21],[22]. A multiple channels actuator can bend bi-directional motion by combining two channels [23] or bend in three directions by combining three channels by 120-degree [24],[25], bend and rotate with three channels for finger-like motion [26], or with four channels in a 90-degree direction [27]. The rotational motion of the SPA facilitates actions such as turning handles, altering the orientation of objects, adjusting items during packaging operations, and twisting to pick fruits, thereby enabling its use in a wide range of applications. However, a fiber-reinforced actuator that limits expansion by winding a wire has a disadvantage: it requires high pressure for complete bending operations. The bending direction, adjusted based on the wire's winding direction or the shape of a channel, provides only one degree of freedom when using a single chamber. Utilizing multiple channels necessitates additional mechanical components,

Manuscript received: December 13, 2023; Revised January 18, 2024; Accepted March 5, 2024.

This paper was recommended for publication by Editor Cecilia Laschi upon evaluation of the Associate Editor and Reviewers' comments.

This work was supported by the National Research Foundation of Korea (NRF) grant funded by the Korea government (MSIT) (NO.2020R1C1C1012279). This work was supported by DGIST R&D program of the Ministry of Science and ICT (23-PCOE-02) *(Corresponding author: Dongwon Yun.)*

The authors are with the Department of Robotics and Mechatronics Engineering, DGIST, Daegu 42988, Republic of Korea (e-mail: y1k1000@dgist.ac.kr; longerthanu@dgist.ac.kr; mech@dgist.ac.kr).

Digital Object Identifier (DOI): see top of this page.

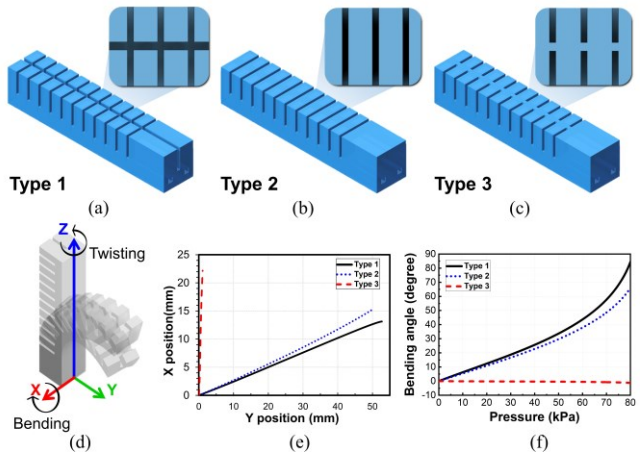

Fig. 1. (a) (b) (c) Designing of three types of TPAs and FEA results of TPAs for twisting and bending, these model have different middle wall positions and chamber shapes: (d) Coordinate axis setting for a two-chamber soft actuator and direction definition for bending and twisting, (e) Position graph for the tip when pressure is applied to one chamber for three designs (f) Graph showing relationship between pressure and bending angles for three designs

such as solenoid valves, airlines, and control elements, which complicates the pneumatic system. Consequently, this leads to an increase in the size of the pneumatic system, hindering miniaturization. Among various SPAs, the PneuNet actuator features a corrugated bellow shape within its pneumatic chamber, which is bonded to flexible yet limited expansion elements. These elements support the actuator's bending motion. As a result, it can achieve greater bending at the same pressure compared to other Soft Pneumatic Actuators [21]-[23],[28]-[35].

Conventional PneuNet actuators have expansion limit layers [28]-[30],[32],[34] which can obtain more tip force by limiting the expansion of the bottom. However, other motions such as rotation are hindered by the expansion limit layer when configured with multiple channels.

In this study, we propose a two-chamber PneuNet actuator (TPA) to which the expansion limit line (ELLINE) is applied to obtain a force gain without a rotational motion limitation due to the expansion limit layer. In the presence of the expansion limit layer, the actuator's rotational motion is inhibited. The ELLINE is thus designed to minimize the influence on twisting by attaching nylon that prevents expansion to the center of rotation and acts as a force enhancement layer similar to the expansion limit layer. We propose three types of SPAs that can rotate, and bend using two channels and perform a finite element analysis (FEA) on these three designs to find the optimal design for twisting and bending under the same pressure. We then confirm the effects on twisting, bending, and tip force according to the width of the ELLINE on the selected design through an FEA. After measuring rotation and bending for the fabricated actuator with and without the ELLINE, the results were compared with the FEA results, and the effect on the tip force and grasping force was investigated. Furthermore, we fabricated a gripper using three-actuator, which has an ELLINE. The performance of the gripper is verified by

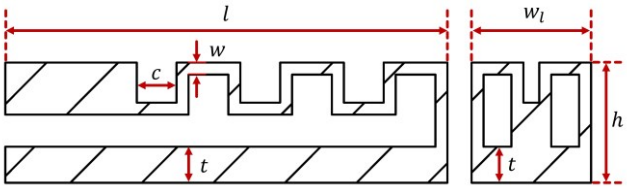

Fig. 2. Cross-section of two-chamber PneuNet actuator.

TABLE I
PARAMETERS OF PNEUNET ACTUATOR

Parameter	
wall thickness (w)	1.5 mm
gap between channels (c)	1.5 mm
gap between chamber (c_b)	1.5 mm
bottom layer thickness (t)	3 mm

conducting grasping experiments for various objects and weights and rotational motion experiments.

II.DESIGN SELECTION OF TPA

A. Finite element analysis of TPA with various shapes

In this section, we propose three designs of TPAs consisting of two channels. These designs can bend when pressure is applied to both channels and rotate when pressure is applied to one chamber. An actuator capable of performing two distinct motions at low pressure was selected, utilizing the structure of the conventional PneuNet actuator. As shown in Fig. 1, the three types of designs have different middle wall positions and chamber shapes. FEA simulations were conducted to assess the impact of the dividing segmented chamber walls on bending and rotation, with all three designs sharing the same internal structure, as shown in Fig. 2. Type 1 has no middle wall between two channels (Fig. 1(a)) [23], Type 2 has a middle wall only in the channel (channel inside the bellows part) (Fig. 1(b)), and Type 3 has a middle wall along the entire length (Z direction) (Fig. 1(c)). Type 2 was designed to resemble the shape of the existing PneuNet actuator [28],[29]. Type 3 is specialized for left and right bending motion, as mentioned in Marchese *et al*. and Schiller *et al*. [13],[36]. Type 3 adds a bottom with the same thickness as Types 1 and 2 to bend in the Y direction.

The bending optimization parameters for the pressure of the PneuNet actuator include wall thickness, the gap between channels, bottom layer thickness, and the cross-sectional shape of the PneuNet actuator, which are discussed in Hu *et al*. [39]. These parameters are applied to the three types of designs and are shown in Fig. 2 and Table I.

A finite element analysis (FEA) using ANSYS Workbench 2021 R1(ANSYS Inc, Pennsylvania, USA) was performed for the three types of designs. The material was silicone with a hardness of 20A, a hyperelastic design with a neo-Hookean design, and a modulus μ = 0.16984 [40],[41]. Through a convergence test, error within 1% of the element size between 1.6 and 1.7 mm was confirmed. Therefore, the element size was selected as 1.6 mm.

The bending angle is defined as the angle measured between the Z-axis and the end points of the soft actuator.

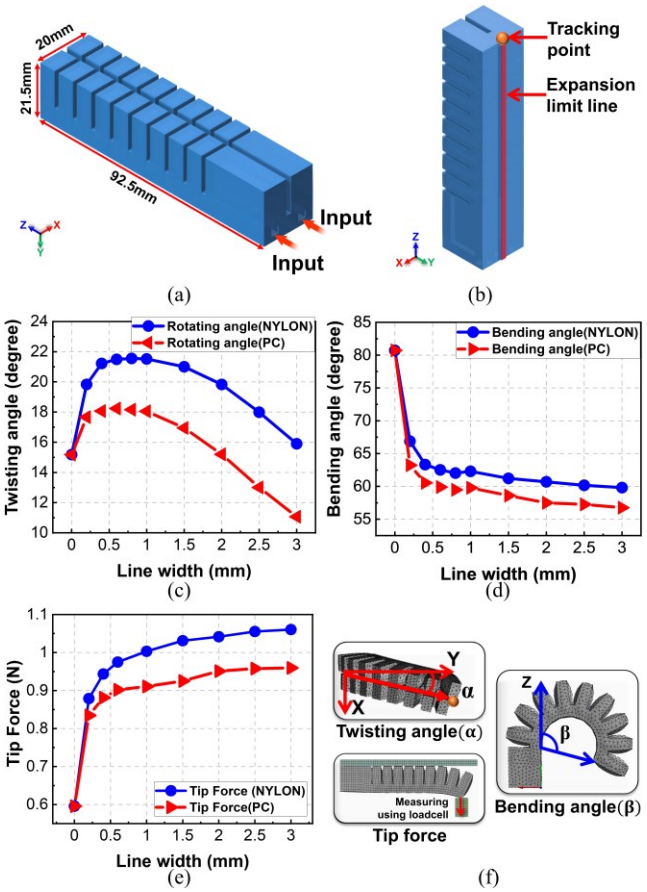

Fig. 3. (a) (b) Model of type 1 TPA with the two material ELLINE and FEA results according to width of the ELLINE when 0 ~ 50 kPa pressure of type 1 TPA is applied: (c) Maximum twisting angle (d) Maximum bending angle, (e) Tip force when 50 kPa is applied. (f) The definitions of twisting, bending angle and tip force.

The definition of the twisting angle is represented by the angle formed between the end points of the soft actuator and the Y-axis. The definitions of these angles can be seen in Fig. 3(f).

FEA results for the three designs are shown in Fig. 1(e) and 1(f). When a pressure of 0~80 kPa was input to one chamber, it was confirmed that all three designs rotated. The maximum twisting angle of each design can be obtained from the tip position, and it was confirmed that Type 1 has a value of 14.3 degrees, Type 2 17.3 degrees, and Type 3 87.5 degrees. The maximum bending angle of each design is 84.5 degrees for Type 1, 66 degrees for Type 2, and 1.45 degrees for Type 3. Type 3 has the widest rotation range at 0~80 kPa input pressure, followed by Type 2 and Type 1. However, Type 3 does not have two degrees of freedom because the maximum bending angle of 1.45 degrees is insufficient for the bending motion. In Type 3 actuators, the presence of a middle wall causes the chambers to move in a way that produces lateral bending, resulting in a significant twisting angle. However, this same middle wall restricts the bending angle, making it smaller. It was anticipated that Type 3 would achieve bending by incorporating a base into the actuators, as seen in the designs by Marchese *et al*. and Schiller *et al*. [13],[36]. Nevertheless, because these actuators were originally designed for bi-directional motion, Type 3 exhibited a smaller bending angle despite achieving a large twisting angle. The difference in the rotation angle between Type 1 and Type 2 is three degrees: Type 1 bends 18.5 degrees more than Type 2. Type 3 has a wide twisting range but a limited bending range of 1.45 degrees. It was confirmed through the FEA that Type 1 and Type 2 had similar maximum twisting angles, but the bending range of Type 1 was larger than that of Type 2. Therefore, Type 1 was selected among the three designs, and the ELLINE was attached to Type 1, as shown in Fig. 3(b).

B. Finite element analysis of TPA with the ELLINE

When an expansion limit layer attached to the existing SPA [28]-[30],[32],[34] rotates, a sufficient twisting angle cannot be obtained because the layer restricts the motion. Since the ELLINE has a small width compared to the layer, it will have a small effect on the rotation. Therefore, by attaching the ELLINE to the Type 1 TPA, we checked the effect of the ELLINE on the operation through an FEA. We used an FEA to simulate the performance according to the ELLINE width of Type 1. Fig. 3(b) is a design when the ELLINE of Type 1 is attached. It was assumed that nylon and polycarbonate, materials used to restrict the deformation of the soft actuator, were attached during this process [37],[38]. Fig. 3(c) is a graph showing the maximum twisting angle (α) according to the width of the ELLINE when a pressure of 0 to 50 kPa is applied to the actuator. Fig. 3(d) is a graph showing the maximum bending angle (β) according to the width of the ELLINE when pressure is applied to the actuator. Fig. 3(e) is a graph showing the FEA results of the tip force according to the width of the ELLINE when 50 kPa is applied to the actuator. In Fig. 3(c), when the width of the ELLINE is 1 mm, both materials exhibit the greatest rotation. It was confirmed that the larger the width was in a range from 0 to 1 mm, the more the maximum twisting angle increased, and the maximum twisting angle then decreased after 1 mm. When the width of the ELLINE is 3 mm, the twisting angle increases compared with no

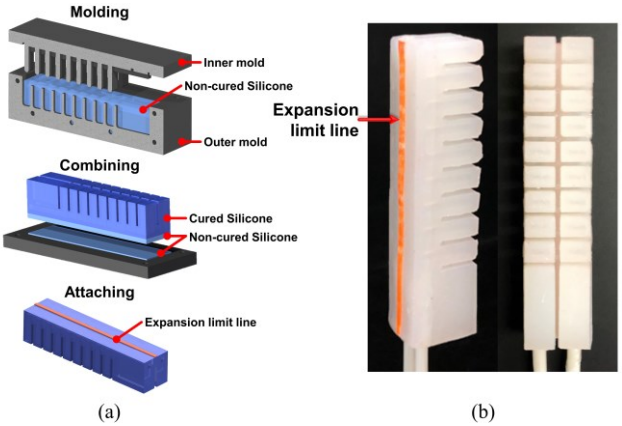

Fig. 4. (a) TPA with fabrication steps and (b) Fabricated TPA with the ELLINE.

ELLINE. When the width is 1 mm, which provides the greatest rotation angle, when material is nylon, the twisting angle increases by 42.0%. In Fig. 3(d), the bending angle was the greatest without the ELLINE, and it was confirmed that the bending angle increased as the line width decreased. When compared to the absence of an ELLINE, it can be observed that both materials exhibit a reduction in bending angle. In Fig. 3(e), when material is nylon the tip force increased by 47.5% with the 0.2 mm line and by 78.0% with the 3 mm line, compared to the case with no ELLINE. In this study, we focused on the force enhancement of the TPA through the ELLINE. We selected the design with the largest rate of increase of tip force among the ELLINE. For polycarbonate, the results showed a 5% smaller bending angle, 20% less rotation angle, and a 5% lower tip force compared to nylon. This indicates that due to its higher stiffness compared to nylon, Polycarbonate requires more moment for bending, leading to a lower performance than nylon when subjected to the same pressure. Therefore, 1 mm nylon, which exhibited greater rotation and a significant increase in force upon attachment, was selected.

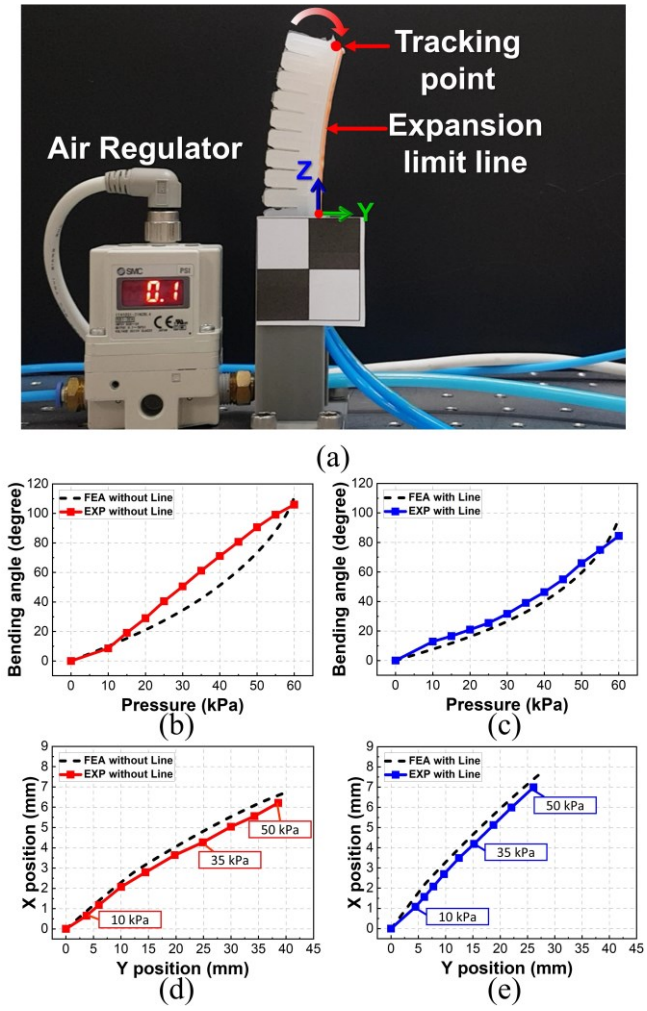

Fig. 5. (a) Setup for the TPA bending and twisting experiments, (b) Comparison of bending experiment and FEA without the ELLINE, (c) Comparison of bending experiment and FEA with the ELLINE,

TABLE II
BENDING AND TWISTING STANDARD ERROR OF EXPERMENT RESULT

Pressure	Bending without line	Bending with line	Twisting without line	Twisting with line
10	1.87	1.39	0.26	0.97
15	2.05	1.46	0.75	0.72
20	1.09	1.06	1.28	0.79
25	0.52	0.98	1.32	0.66
30	0.94	1.58	1.15	0.55
35	0.73	1.07	0.92	0.26
40	2.39	1.96	1.18	0.42
45	0.99	2.02	1.18	0.15
50	1.82	1.64	0.81	0.32
55	1.54	2.19	-	-
60	1.06	1.51	-	-
Average	1.87	1.39	0.26	0.97

III. TPA WITH THE ELLINE FABRICATION

The mold was designed for the fabrication of a TPA using a 3D printer (M300, Zortrax), and silicone rubber (XINUS SH3264, XINUSLAB, shore hardness 20A) was injected into the mold, as shown in Fig. 4(a). The mold consists of a total of five parts and is largely divided into a bottom part and an actuator part. The fabrication process consists of four steps. First, the actuator part mold with silicone rubber is placed in an oven at 80 °C to cure it for 20 minutes. The silicone actuator part is then removed from the mold. Second, the silicone actuator part is placed on top of the uncured bottom part and heated in an oven to attach it to the bottom part. The bottom part was fabricated by increasing the width by 1 mm for easy attachment. For tube connection, a 4 mm polyurethane tube with uncured silicone is inserted into the cured TPA and cured in an oven. Third, using an adhesive for silicone, a nylon wire is attached to the back of the actuator to make an ELLINE with a width of 1 mm. In the final step, the completed actuator is placed in water to check if air is leaking, and uncured silicone is added to the leaking parts and cured after that, the fabricated TPA is shown in Fig. 4(b).

IV. TPA EXPERIMENT RESULTS

A. Bending and rotation experiments of TPA

Fig. 5(a) shows the setup of the experiment to measure the bending and twisting of the TPA. To observe the bending and twisting of the TPA, it was installed vertically, and the experiment was recorded through a camera. Each experiment was conducted five times. To supply constant pressure, an electronic pneumatic regulator (ITV1031-21N2BL, SMC co.) was used, and an image processing program (Tracker, Open Source Physics) was used to track the fingertip trajectory of the TPA fixed in a base. The markers in Fig. 5(b) and Fig. 5 (c) have intervals of 10 kPa when 0 to 60 kPa is applied in the TPA. Fig. 5(b) shows a comparison between the experiment and the FEA for the bending angle without the ELLINE when pressure is applied to the two channels. The results of the bending experiment and the FEA with the ELLINE are compared in Fig. 5(c). Fig. 5(d) shows a comparison between the experiment and the FEA for the trajectory of the actuator tip applied the

pressure to only one chamber, without the ELLINE in the XY plane when 0 to 50 kPa. A comparison between the experiment and the FEA for the trajectory of the actuator tip with the ELLINE in the XY plane is shown Fig. 5(e) when 0 to 50 kPa. At the same pressure, the maximum twisting angle was 11.9 degrees without the ELLINE and 15.5 degrees with the ELLINE. It was confirmed that in the case with the ELLINE at the same pressure, the maximum twisting angle increased by 22.8%. In addition, it was confirmed that the bending angle was reduced by up to 21.1 degrees and 19.8% compared to the case without the ELLINE at the same pressure.

The error between the FEA results for the bending and the experiment, with an error of 11.4% with the ELLINE and 19.2% without the ELLINE and standard error was 2.39 and 1.96, respectively. The error between the FEA results for bending and the experiment was 8.7% with the ELLINE and 8.8% without the ELLINE and the standard error was 0.26 and 0.92. The standard error of bending and twisting experiment results is shown in Table II. From the FEA simulations and experiments, it was observed that attachment of the ELLINE can increase the angle of rotation and decrease the angle of bending.

B. Tip force and grasping force experiment of a TPA.

Fig. 6(a) shows the experimental setup to investigate the effects of the tip force according to with and without the ELLINE. When the TPA was fixed in a vise and the pressure was increased at 10 kPa intervals in the range of 0 to 70 kPa, the magnitude of the tip force was measured with a loadcell

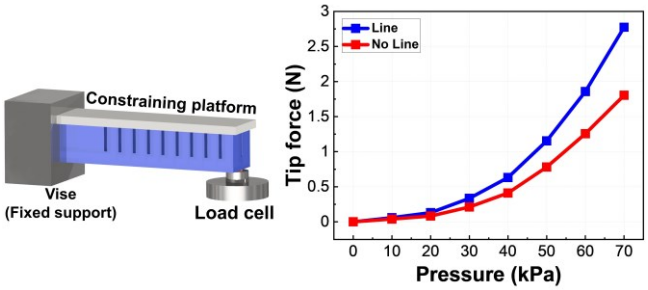

(a) (b)

Fig. 6. (a) Setup for tip force experiment of the TPA and (b) experiment results of tip force with and without the ELLINE.

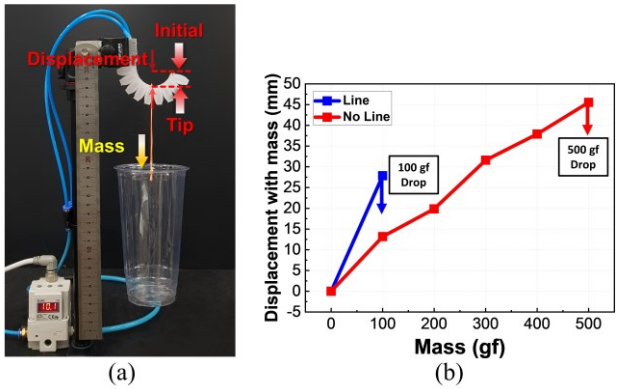

(a) (b)

Fig. 7. (a) Setup for grasping force experiment of the TPA and (b) Mass vs. displacement of the TPA with and without the ELLINE.

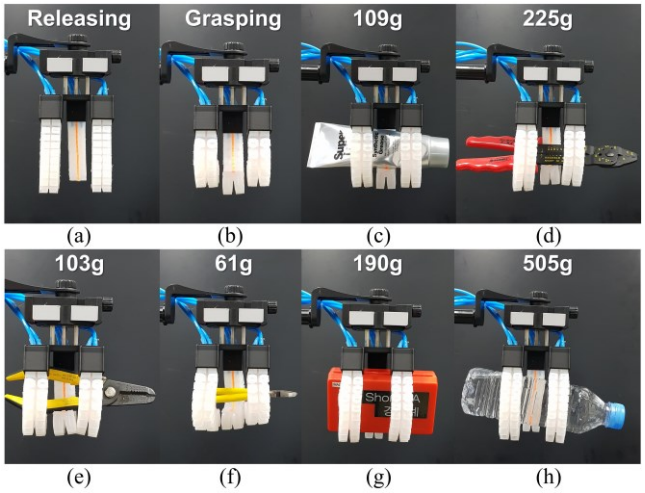

Fig. 8. Grasping experiment of two-chamber soft gripper and six objects: (a) gripper releasing, (b) gripper grasping, (c) grease tube, (d) large wire stripper, (e) wire stripper, (f) nipper, (g) plastic case, (h) plastic bottle.

repeatedly five times. Constraining the top surface of the actuator minimized the non-linear effects caused by the bending of the actuator when pressurized. Thus, this setup could measure the maximum blocked tip force generated by the actuator regardless of the bending angle [11]. The results confirmed that the average tip force was 2.78 N and 1.80 N with and without the ELLINE, respectively, in the error range of 0.0477 N at an input pressure of 70 kPa (Fig. 6(b)). It was 1.54 times greater tip force obtained in the TPA with the ELLINE.

The experimental setup (Fig. 7(a)) for measuring the deformation of the TPA depending on the load. The initial position of the TPA tip was set when bent beyond 90 degrees to form a semi-circular shape under an input pressure of 70 kPa with no load applied. The mass is always placed in the center of the actuator. The distance between the end position with the applied load and the initial position of the soft actuator was measured using an image processing program (Tracker, Open Source Physics), as shown in Fig. 7(b). The TPA deformed 27.9 mm and slid with a load of 100 g without the ELLINE and deformed 45.5 mm and slid with a load of 500 g with the ELLINE. It has been demonstrated that, when installed in the direction of gravity and subjected to the same pressure, the TPA with the ELLINE could support a load five times greater than without the ELLINE.

These results confirm that, with the ELLINE, it is possible to obtain a greater force by limiting the expansion of the bottom part and obtaining more stiffness against external forces of the bottom part. Simplifying a TPA as a beam with a free end subjected to a bending moment, the bending moment of TPA M is as follows: $M = \frac{EI}{\mathrm{R}}$ [32],[42]. The Young's modulus E and moment of inertia I, the bending radius R. Nylon has a Young's modulus about 1900 times greater than that of pure silicone rubber. Therefore, the TPA with attached nylon has a larger E than an unattached TPA. The attached TPA can hold higher loads against external forces. The bottom is easily deformed and cannot hold a large load without the ELLINE when external force is

applied. However, the TPA with the ELLINE can hold a large load by preventing deformation of the bottom.

C. Grasping and rotational motion experiment of soft gripper

To apply pressure to the actuator, a small air pump (DAP-8849, Motorbank) that can apply a maximum pressure of 300 kPa and a pneumatic regulator (ITV1031-21N2BL, SMC co.) to keep the pressure constant were used. As depicted in Fig. 8(a), we fabricated a gripper comprising three TPAs with ELLINE, arranged in parallel, and positioned the gripper in the direction of gravity. The distance between each actuator is designed to be 70 mm. The gripper was fabricated with a Z-HIPS filament and a 3D printer (M300, Zortrax). The grasping experiment was conducted by holding six various objects in three categories: cylinder type, cuboid type, and tool. In this experiment, cylindrical objects such as a plastic bottle, grease tube, cuboid objects such as plastic cases, tools such as wire strippers, and nipper were used. At 70 kPa, the gripper can successfully hold plastic bottle with weights of up to 505 g and curved objects such as cylindrical grease tube (109 g), hexahedral plastic cases (190 g), and tools (225 g), as shown in Fig. 8. It was confirmed through an experiment that the motion range of the fingertip is 36 mm with the ELLINE. Also, since the distance between the actuators of the gripper was 70 mm, it was confirmed that it was possible to hold objects with size in a range of 36 mm to 70 mm.

Fig. 9 shows images taken at one-second intervals when pressure is applied to one chamber in the same direction to check whether the soft gripper can perform the rotational motion. When the pressure of 75 kPa was applied to one chamber of the TPA, it was confirmed that the TPA rotated in one direction to turn the object while holding the 32 mm cylindrical column. By repeating ten times and recording the angle and time for one operation, the results shown in Table III were obtained. In one operation, the average rotating angle was 44.3 degrees, the average operation time was 3.61 seconds, the standard deviation for the rotating angle was 8.64, and the standard deviation for the average operation time was 0.465. The results of the rotational motion experiment confirmed that the soft gripper consisted of three actuators can rotate the object at a speed of 12.3 degrees/sec.

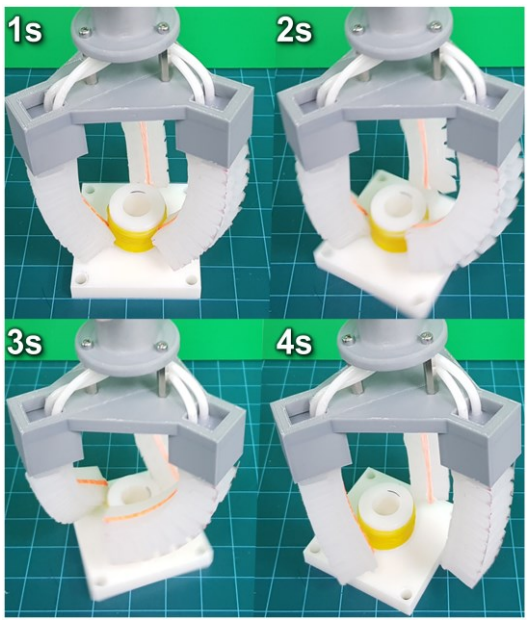

Fig. 9. Rotational motion experiment of soft gripper.

TABLE III
TIME MEASUREMENT RESULTS FOR ROTATIONAL MOTION OF THE GRIPPER AND TWISTING ANGLE

Try	Degree	Time
1	36.9	4
2	33.8	4
3	49.3	3.8
4	57.7	4.4
5	40.5	3.9
6	45.3	3.2
7	50.1	3.2
8	30.3	3.3
9	49.9	3
10	49.4	3.3
Average	44.3	3.61

In addition to cylinders, we experimented with rotational motion with various objects on the platform. These included a paper cup with a 100g weight (⌀80 mm), a tangerine (⌀64 mm), a pencil holder (width 70 mm), and a hemisphere model (⌀27 mm). It was confirmed that these objects could be rotated and lifted up, as demonstrated in the Supplementary Video.

V. CONCLUSION

In this study, we propose three designs using a TPA that can bend and rotate. We selected a suitable design for bending and twisting through an FEA. Through simulations, the twisting angle, bending angle, and tip force for the selected design without the ELLINE and with an ELLINE with width from 0.2 to 3 mm were compared. The case with the ELLINE confirmed a 4.74%~42% increase in the maximum twisting angle compared to the case without the ELLINE. We confirmed that the tip force increased the force by 47.5%~78.0% in the case with the ELLINE. However, it was confirmed that the bending angle decreased by 17.16%~26% compared to the case without the ELLINE.

In other words, the twisting angle and tip force of the TPA with the ELLINE increased, but the bending angle decreased. As the ELLINE width becomes thicker, the bending angle decreases, and the tip force increases. This phenomenon seems to arise from the reduced deformation in the silicone bottom as the width of ELLINE increases, which leads to increased stiffness of the silicone bottom. This enhancement allows for a more efficient transfer of the moment. Consequently, with the material attached to the bottom remaining the same, the wider the ELLINE attached to the TPA, the greater the tip force obtained under the same input pressure, instead of decreasing the deformation. In the case of the twisting angle, it has the maximum rotation angle when it is 0.8 mm. The twisting angle increases as the width increases before an ELLINE width of 0.8 mm. After 0.8 mm, the rotation angle decreases as the width increases. In this study, we focused on the force enhancement of the TPA through the ELLINE. Therefore, the 1 mm line design with nylon, where the rate of increase of the maximum twisting angle was 30.11%, the rate of decrease of the maximum

bending angle was 24.80%, and the rate of increase of the tip force was 74.84%, was selected and fabricated for an experiment to assess its performance. The error between the FEA results for bending and the experiment was 8.7% with the ELLINE and 8.8% without the ELLINE. The error between the FEA results for bending and the experiment was 11.4% with the ELLINE and 19.2% without the ELLINE. The bending angle in the case with the ELLINE decreased by 19.8% in the experiment. The twisting angle increased by 22.8% in the experiment at the same pressure in the case with the ELLINE. The experiment results confirmed that when the 1 mm ELLINE was attached to the fabricated actuator, the twisting angle increased, and the bending angle decreased compared to the actuator without the ELLINE.

When the TPA has the ELLINE, the tip force is 1.58 times greater at the same pressure, the grasping force is up to five times higher than without ELLINE. This prevents the deformation of the bottom due to the stiffness of the ELLINE. Thus, it is possible to obtain greater stiffness against external force than without the ELLINE. The TPA with the ELLINE can hold a large load by preventing deformation of the bottom.

Table IV shows the calculated tip force per unit of pressure for a total of 10 existing PneuNet actuators [21],[23],[28]-[35]. The TPA with an ELLINE has a value of 0.0397 N/kPa, which is the highest among the 10 existing PneuNet actuators. The proposed actuator has the advantage of operating at a low pressure of under 100 kPa in contrast to the actuator in Li *et al*. [31] that operates at a high pressure of 400 kPa. Furthermore, the proposed actuator can hold and rotate objects through bending and twisting with two degrees of freedom, similar Abondance *et al*. [23]'s actuator. The actuator in this study has low operating pressure and exhibits a greater increase in tip force per unit of pressure compared to the actuator studied by Abondance *et al*. [23].

TABLE IV
COMPARISON OF PRESSURE VS TIP FORCE AND INNER VOLUME OF EXISTING PNEUNET ACTUATORS

Authors	Motion	Tip force(N) /Pressure(kPa)	Inner Volume (mm^3)	Length (mm^2)
Our research	Bending twisting	0.0397	3159	92.5
S. Abondance *et al.* [23]	Bending twisting	0.0092	-	100
Z. Liu *et al.* [30]	Bending	0.0198	-	48
H. Li *et al.* [31]	Bending	0.0375	-	-
G. Alici *et al*.[32]	Bending	0.029	6480	140
P. Polygerinos *et al.* [28]	Bending	0.028	-	136
Z. Sun *et al.* [33]	Bending	0.025	-	123
B. Mosadegh *et al.* [29]	Bending	0.019	3021	86
J. Wang *et al.* [34]	Bending	0.010	4914	174
W. Hu *et al.* [21]	Helical	0.009	-	150
J. H. Low *et al.* [35]	Bending	0.0084	-	156

We fabricated a soft gripper, and a grasping experiment was conducted on a total of six types of cylindrical and cuboid objects and tools. It succeeded in grasping up to 505 g plastic bottle and in grasping objects with complex shapes such as tools. The rotational motion experiment on a cylindrical object through the twisting of the actuator was conducted ten times and it was confirmed that the soft gripper consisting of three actuators can rotate the object at a speed of 12.3 degrees/sec. And it was confirmed that the gripper could rotate and lift objects. The gripper is expected to facilitate actions such as turning handles, altering the orientation of objects, adjusting items during packaging operations, and twisting to pick fruits.

For the material limiting the expansion of the proposed actuator, we selected nylon and polycarbonate, both of which have been utilized in previous soft actuator research, for our simulations. The simulation results confirmed that nylon, due to its lower stiffness, leads to better actuator performance. Beyond just these two materials, it's crucial to further explore how actuator performance is influenced by employing materials with varying stiffness levels as the ELLINE.

We confirmed that these objects could be rotated and lifted, as demonstrated in the Supplementary Video. However, when turning objects in the air, there was difficulty in rotating them stably due to the edges of the fingertips. This issue is expected to be addressed by modifying the shape of the actuator's tip to a rounded form through future studies.

The gripper deforms to fit the shape of the object to ensure a stable grasp. However, there was a limitation in the size of the object with respect to the size of the gripper and the length of the actuator. For an object smaller than the length of the actuator being used, only a size range larger than the minimum curvature of the actuator can be grasped. There was also a limitation due to the slow operating speed of the gripper. In future studies, we plan to address the size limit problem of the objects that can be grasped by developing actuators with variable lengths or by implementing a mode change for the gripper. The slow operating speed problem of the gripper is intended to be resolved through research on the material or structural aspects of the actuator.

REFERENCES

[1] Y. Kang, D. Kim, and D. Yun, "Manipulator Collision Avoidance System Based on a 3D Potential Field With ISO 15066," *IEEE Access*, vol. 10, pp. 126593–126602, 2022

[2] G. Alici, "Softer is Harder: What Differentiates Soft Robotics from Hard Robotics?" *MRS Advances*, vol. 3, no. 28, pp. 1557–1568, Jun. 2018

[3] J. Shintake, V. Cacucciolo, D. Floreano, and H. Shea, "Soft Robotic Grippers," *Adv. Mater.*, vol. 30, no. 29, p. 1707035, Jul. 2018.

[4] I. Ju and D. Yun, "Hydraulic variable stiffness mechanism for swimming locomotion optimization of soft robotic fish," *Ocean Engineering*, vol. 286, p. 115551, Oct. 2023

[5] Y. Yang, Y. Chen, Y. Li, M. Z. Q. Chen, and Y. Wei, "Bioinspired Robotic Fingers Based on Pneumatic Actuator and 3D Printing of Smart Material," *Soft Robotics*, vol. 4, no. 2, pp. 147–162, Jun. 2017.

[6] J. Jeong, I. B. Yasir, J. Han, C. H. Park, S.-K. Bok, and K.-U. Kyung, "Design of Shape Memory Alloy-Based Soft Wearable Robot for Assisting Wrist Motion," *Applied Sciences*, vol. 9, no. 19, p. 4025, Sep. 2019.

[7] J. Shintake, S. Rosset, B. Schubert, D. Floreano, and H. Shea, "Versatile Soft Grippers with Intrinsic Electroadhesion Based on Multifunctional Polymer Actuators," *Adv. Mater.*, vol. 28, no. 2, pp. 231–238, Jan. 2016.

[8] G. Alici and N. N. Huynh, "Performance Quantification of Conducting Polymer Actuators for Real Applications: A Microgripping System," *IEEE/ASME Trans. Mechatron.*, vol. 12, no. 1, pp. 73–84, Feb. 2007.

[9] S. McGovern, G. Alici, V.-T. Truong, and G. Spinks, "Finding NEMO (novel electromaterial muscle oscillator): a polypyrrole powered robotic fish with real-time wireless speed and directional control," *Smart Mater. Struct.*, vol. 18, no. 9, p. 095009, Sep. 2009

[10] J.-W. Kim, K. Yoshida, K. Kouda, and S. Yokota, "A flexible electro-rheological microvalve (FERV) based on SU-8 cantilever structures and its application to microactuators," *Sensors and Actuators A: Physical*, vol. 156, no. 2, pp. 366–372, Dec. 2009.

[11] P. Polygerinos *et al.*, "Modeling of Soft Fiber-Reinforced Bending Actuators," *IEEE Trans. Robot.*, vol. 31, no. 3, pp. 778–789, Jun. 2015.

[12] P. H. Nguyen, F. Lopez-Arellano, W. Zhang, and P. Polygerinos, "Design, Characterization, and Mechanical Programming of Fabric-Reinforced Textile Actuators for a Soft Robotic Hand," in *2019 IEEE/RSJ International Conference on Intelligent Robots and Systems (IROS)*, Macau, China: IEEE, Nov. 2019, pp. 8312–8317.

[13] A. D. Marchese, R. K. Katzschmann, and D. Rus, "A Recipe for Soft Fluidic Elastomer Robots," *Soft Robotics*, vol. 2, no. 1, pp. 7–25, Mar. 2015.

[14] J. Walker *et al.*, "Soft Robotics: A Review of Recent Developments of Pneumatic Soft Actuators," *Actuators*, vol. 9, no. 1, p. 3, Jan. 2020.

[15] A. D. Marchese, C. D. Onal, and D. Rus, "Autonomous Soft Robotic Fish Capable of Escape Maneuvers Using Fluidic Elastomer Actuators," *Soft Robotics*, vol. 1, no. 1, pp. 75–87, Mar. 2014.

[16] K. H. L. Heung, R. K. Y. Tong, A. T. H. Lau, and Z. Li, "Robotic Glove with Soft-Elastic Composite Actuators for Assisting Activities of Daily Living," *Soft Robotics*, vol. 6, no. 2, pp. 289–304, Apr. 2019.

[17] C. Correia *et al.*, "Improving Grasp Function After Spinal Cord Injury with a Soft Robotic Glove," *IEEE Trans. Neural Syst. Rehabil. Eng.*, vol. 28, no. 6, pp. 1407–1415, Jun. 2020.

[18] D. Drotman, S. Jadhav, M. Karimi, P. de Zonia, and M. T. Tolley, "3D printed soft actuators for a legged robot capable of navigating unstructured terrain," in *2017 IEEE International Conference on Robotics and Automation (ICRA)*, Singapore: IEEE, May 2017, pp. 5532–5538.

[19] Z. Wang, P. Polygerinos, J. T. B. Overvelde, K. C. Galloway, K. Bertoldi, and C. J. Walsh, "Interaction Forces of Soft Fiber Reinforced Bending Actuators," *IEEE/ASME Trans. Mechatron.*, vol. 22, no. 2, pp. 717–727, Apr. 2017.

[20] P. Polygerinos, K. C. Galloway, E. Savage, M. Herman, K. O. Donnell, and C. J. Walsh, "Soft robotic glove for hand rehabilitation and task specific training," in *2015 IEEE International Conference on Robotics and Automation (ICRA)*, Seattle, WA, USA: IEEE, May 2015, pp. 2913–2919.

[21] W. Hu and G. Alici, "Bioinspired Three-Dimensional-Printed Helical Soft Pneumatic Actuators and Their Characterization," *Soft Robotics*, vol. 7, no. 3, pp. 267–282, Jun. 2020.

[22] T. Wang, L. Ge, and G. Gu, "Programmable design of soft pneu-net actuators with oblique chambers can generate coupled bending and twisting motions," *Sensors and Actuators A: Physical*, vol. 271, pp. 131–138, Mar. 2018.

[23] S. Abondance, C. B. Teeple, and R. J. Wood, "A Dexterous Soft Robotic Hand for Delicate In-Hand Manipulation," *IEEE Robot. Autom. Lett.*, vol. 5, no. 4, pp. 5502–5509, Oct. 2020.

[24] R. V. Martinez *et al.*, "Robotic Tentacles with Three-Dimensional Mobility Based on Flexible Elastomers," *Adv. Mater.*, vol. 25, no. 2, pp. 205–212, Jan. 2013.

[25] B. Zhang, C. Hu, P. Yang, Z. Liao, and H. Liao, "Design and Modularization of Multi-DoF Soft Robotic Actuators," *IEEE Robot. Autom. Lett.*, vol. 4, no. 3, pp. 2645–2652, Jul. 2019.

[26] K. Batsuren and D. Yun, "Soft Robotic Gripper with Chambered Fingers for Performing In-Hand Manipulation," *Applied Sciences*, vol. 9, no. 15, p. 2967, Jul. 2019.

[27] Z. Chen, X. Liang, T. Wu, T. Yin, Y. Xiang, and S. Qu, "Pneumatically Actuated Soft Robotic Arm for Adaptable Grasping," *Acta Mech. Solida Sin.*, vol. 31, no. 5, pp. 608–622, Oct. 2018.

[28] P. Polygerinos *et al.*, "Towards a soft pneumatic glove for hand rehabilitation," in *2013 IEEE/RSJ International Conference on Intelligent Robots and Systems*, Tokyo: IEEE, Nov. 2013, pp. 1512–1517.

[29] B. Mosadegh *et al.*, "Pneumatic Networks for Soft Robotics that Actuate Rapidly," *Adv. Funct. Mater.*, vol. 24, no. 15, pp. 2163–2170, Apr. 2014.

[30] Z. Liu, F. Wang, S. Liu, Y. Tian, and D. Zhang, "Modeling and Analysis of Soft Pneumatic Network Bending Actuators," *IEEE/ASME Trans. Mechatron.*, vol. 26, no. 4, pp. 2195–2203, Aug. 2021.

[31] H. Li, J. Yao, P. Zhou, X. Chen, Y. Xu, and Y. Zhao, "High-force soft pneumatic actuators based on novel casting method for robotic applications," *Sensors and Actuators A: Physical*, vol. 306, p. 111957, May 2020.

[32] G. Alici, T. Canty, R. Mutlu, W. Hu, and V. Sencadas, "Modeling and Experimental Evaluation of Bending Behavior of Soft Pneumatic Actuators Made of Discrete Actuation Chambers," *Soft Robotics*, vol. 5, no. 1, pp. 24–35, Feb. 2018.

[33] Z. Sun, Z. Guo, and W. Tang, "Design of wearable hand rehabilitation glove with soft hoop-reinforced pneumatic actuator," *J. Cent. South Univ.*, vol. 26, no. 1, pp. 106–119, Jan. 2019.

[34] J. Wang, Y. Fei, and W. Pang, "Design, Modeling, and Testing of a Soft Pneumatic Glove With Segmented PneuNets Bending Actuators," *IEEE/ASME Trans. Mechatron.*, vol. 24, no. 3, pp. 990–1001, Jun. 2019.

[35] J. H. Low *et al.*, "Hybrid Tele-Manipulation System Using a Sensorized 3-D-Printed Soft Robotic Gripper and a Soft Fabric-Based Haptic Glove," *IEEE Robot. Autom. Lett.*, vol. 2, no. 2, pp. 880–887, Apr. 2017.

[36] L. Schiller, A. Seibel, and J. Schlattmann, "Toward a Gecko-Inspired, Climbing Soft Robot," *Front. Neurorobot.*, vol. 13, p. 106, Dec. 2019.

[37] R. V. Martinez, A. C. Glavan, C. Keplinger, A. I. Oyetibo, and G. M. Whitesides, "Soft Actuators and Robots that Are Resistant to Mechanical Damage," *Adv Funct Materials*, vol. 24, no. 20, pp. 3003–3010, May 2014.

[38] M. Fatahillah, N. Oh, and H. Rodrigue, "A Novel Soft Bending Actuator Using Combined Positive and Negative Pressures," *Front. Bioeng. Biotechnol.*, vol. 8, p. 472, May 2020.

[39] W. Hu, R. Mutlu, W. Li, and G. Alici, "A Structural Optimisation Method for a Soft Pneumatic Actuator," *Robotics*, vol. 7, no. 2, p. 24, Jun. 2018.

[40] L. Marechal, P. Balland, L. Lindenroth, F. Petrou, C. Kontovounisios, and F. Bello, "Toward a Common Framework and Database of Materials for Soft Robotics," *Soft Robotics*, vol. 8, no. 3, pp. 284–297, Jun. 2021.

[41] K Larson. "Can You estimate modulus from durometer hardness for silicones." *Dow Corning Corporation*. 2016;1–6".

[42] G. Miron, B. Bédard, and J.-S. Plante, "Sleeved Bending Actuators for Soft Grippers: A Durable Solution for High Force-to-Weight Applications," *Actuators*, vol. 7, no. 3, p. 40, Jul. 2018.